

Delayed Control of a Moore-Greitzer Axial Compressor model

Werner Aernouts*, Dirk Roose

Department of Computer Science, K.U.Leuven
Celestijnenlaan 200 A, B-3001 Heverlee, Belgium
{werner.aernouts, dirk.roose}@cs.kuleuven.ac.be

Rodolphe Sepulchre

Institut Montefiore, B28, Université de Liège
B-4000 Liège Sart-Tilman, Belgium
sepulchre@montefiore.ulg.ac.be

January 6, 1999

Abstract

Several feedback control laws have appeared in the literature concerning the stabilization of the nonlinear Moore-Greitzer axial compression model. Motivated by magnitude and rate limitations imposed by the physical implementation of the control law, Larsen et al. studied a dynamic implementation of the S-controller suggested by Sepulchre and Kokotović. They showed the potential benefit of implementing the S-controller through a first order lag: while the location of the closed-loop equilibrium achieved with the static control law was sensitive to poorly known parameters, the dynamic implementation resulted in a small limit cycle at a very desirable location, insensitive to parameter variations.

In this paper, we investigate the more general case when the control is applied with a time delay. This can be seen as an extension of the model with a first order lag. The delay can either be a result of system constraints or be deliberately implemented to achieve better system behaviour. The resulting closed-loop system is a set of parameter dependent delay differential equations. Numerical bifurcation analysis is used to study this model and investigate whether the positive results obtained for the first order model persist, even for larger values of the delay.

1 Introduction

Two undesirable phenomena, rotating stall and surge, limit the use of an axial compressor near its maximum achievable pressure rise. Rotating stall is characterised by a region of blocked flow that rotates around the annulus of the compressor and forces the compressor to operate at reduced pressure. Surge is characterised by large axisymmetric oscillations.

Moore and Greitzer [6] developed a model for axial compression systems, by taking a one-mode Galerkin approximation of a PDE which relates the pressure rise Ψ , the annulus-averaged mass

*Corresponding author

flow coefficient Φ and the non-axisymmetric flow disturbance. This so-called Moore-Greitzer model consists of the following three nonlinear ODEs [6] :

$$\begin{aligned}\dot{\Phi} &= -\Psi + \Psi_c(\Phi) - 3\Phi R \\ \dot{\Psi} &= \frac{1}{\beta^2}(\Phi + 1 - \sqrt{\Psi}(\Gamma + u)) \\ \dot{R} &= \sigma R(1 - \Phi^2 - R)\end{aligned}\tag{1}$$

where R is the square magnitude of the first Fourier mode of the flow disturbance and $\Psi_c(\Phi)$ is the characteristic of the actual compressor, often (heuristically) described by the following cubic polynomial :

$$\Psi_c(\Phi) = \Psi_0 + 1 + \frac{3}{2}\Phi - \frac{1}{2}\Phi^3.\tag{2}$$

β and σ are parameters whose value is determined by the type and operation mode of the compressor, $\Gamma + u$ is related to the throttle opening, which can be modified by the control variable u . When $u = 0$, the value of the parameter Γ determines the position of the equilibrium points in the uncontrolled model. The value of Γ for which the uncontrolled model has an equilibrium at the point $(1, \Psi_0 + 2, 0)$ is denoted by Γ_{peak} , because this corresponds to the maximal achievable pressure rise. Both R and Ψ can only assume positive values.

The system (1) has two loci of equilibria. One corresponds to steady axisymmetric flow with $R = 0, \Psi = \Psi_c(\Phi)$ and is further referred to as the *no-stall characteristic*. The other corresponds to steady non-axisymmetric flow with $R \neq 0, \Psi = \Psi_c(\Phi) - 3\Phi(1 - \Phi^2)$, further referred to as the *stall characteristic*.

2 S-control with first order lag

In this section we will recall the results obtained by Larsen et al. [4] concerning a dynamic implementation of the so called S-control law [7]. We define the function $\Psi_s(\Phi)$ to be the pressure along the locus of stabilizable equilibria of (1), and $\Psi_u(\Phi)$ to be the pressure along the locus of equilibria that are not stabilizable, i.e.

$$\Psi_s(\Phi) = \begin{cases} \Psi_c(\Phi) & \text{when } \Phi \geq 1 \\ \Psi_c(\Phi) - 3\Phi(1 - \Phi^2) & \text{when } \Phi < 1 \end{cases}$$

and

$$\Psi_u(\Phi) = \Psi_c(\Phi) \text{ when } \Phi < 1.$$

The S-control law [7] is then defined as

$$u = \frac{\Gamma_0 + k(\Psi - \Psi_s(\Phi))}{\sqrt{\Psi}} - \bar{\Gamma},\tag{3}$$

where Γ_0 and $\bar{\Gamma}$ are parameters that determine, for a given Γ , the position of the closed loop equilibrium. The gain k determines how fast the state is driven towards the manifold $\Psi_s(\Phi)$.

Following [7], Larsen et al. assumed that the control entered through a first order lag

$$\chi(s) = \frac{1}{\tau s + 1}u(s),\tag{4}$$

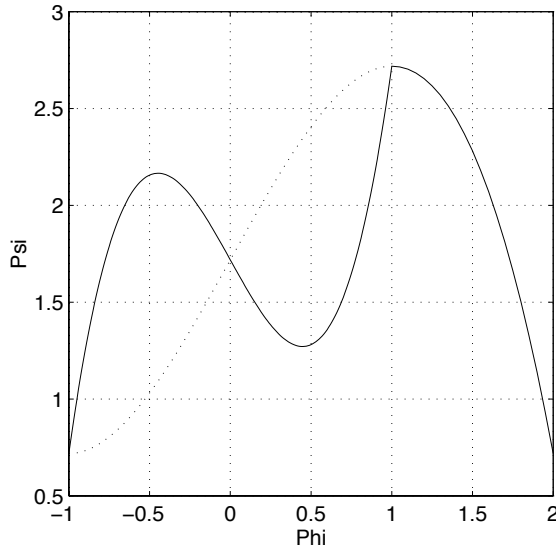
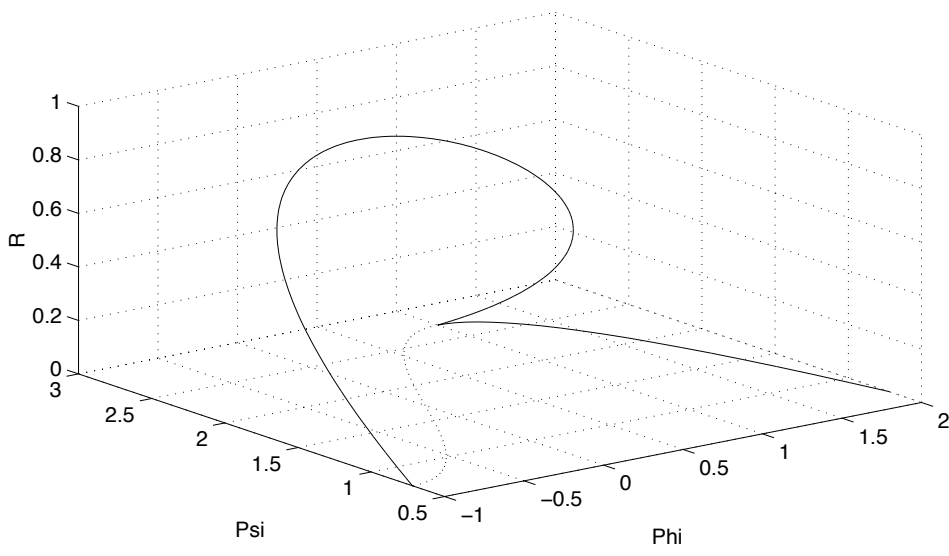


Figure 1: Stabilizable versus not stabilizable equilibria: Ψ_s (full) and Ψ_u (\cdots)

resulting in the system

$$\begin{aligned}
 \dot{\Phi} &= -\Psi + \Psi_c(\Phi) - 3\Phi R \\
 \dot{\Psi} &= \frac{1}{\beta^2}(\Phi + 1 - \sqrt{\Psi}(\Gamma + \chi)) \\
 \dot{R} &= \sigma R(1 - \Phi^2 - R) \\
 \tau \dot{\chi} &= u - \chi.
 \end{aligned} \tag{5}$$

Their analysis leads to the following conclusion [4]: For a fixed value of Γ smaller than Γ_{peak} , there are two equilibria, one on the stall characteristic and one on the no-stall characteristic. When increasing the time constant τ , both equilibria undergo a Hopf bifurcation. This results in two periodic solutions. The one from the stall equilibrium is stable and is located above the $R = 0$ plane. The other periodic

solution is unstable in the R -direction, and is located in the (invariant) $R = 0$ plane. When the time constant τ is increased further, the stable periodic solution moves towards the $R = 0$ plane and undergoes a transcritical cyclic bifurcation where it exchanges stability with the limit cycle in the $R = 0$ plane. For larger values of τ a stable limit cycle in the $R = 0$ plane remains, with excellent physical properties, that is, it is very small in size and is located very close to the peak in the curve $\Psi = \Psi_s(\Phi)$, which corresponds to the maximal achievable static pressure rise. This result ensures that the system (5) is robust with respect to perturbations on Γ , when τ is taken large enough. Because Γ is a poorly known parameter, this is a highly desirable property. In the absence of the first order lag, even a small perturbation of Γ causes the equilibrium point to shift along the stall characteristic.

3 Delayed Control Law

It is an interesting question to ask whether the results from the previous section are typical for the system with first order lag, or are in fact due to some general form of “lagged behaviour”. For this reason, we assume in this paper that the control is applied with a time delay,

$$\chi(t) = u(t - \tau) \tag{6}$$

resulting in

$$\begin{aligned} \dot{\Phi} &= -\Psi + \Psi_c(\Phi) - 3\Phi R \\ \dot{\Psi} &= \frac{1}{\beta^2}(\Phi + 1 - \sqrt{\Psi}(\Gamma + u(t - \tau))) \\ \dot{R} &= \sigma R(1 - \Phi^2 - R) \end{aligned} \tag{7}$$

Equation (6) is equivalent to $u(t) = \chi(t + \tau)$. If we take a Taylor expansion of the right hand side and neglect all but the first two terms, this results in $u(t) = \chi(t) + \tau\dot{\chi}$, which is the last equation of (5) rewritten. In this way, (5) can be seen as a first order approximation of (7).

Note that the system (7) is no longer a set of ODEs, but a set of Delay Differential Equations (DDEs), and that the parameter τ no longer corresponds to a time constant, but to a time delay. In this section, we investigate the dynamical properties of this system by means of a numerical bifurcation analysis.

3.1 Analysis of equilibrium points

We first recall some general properties of solutions of DDEs, which will be used in the analysis of the system (7). To this end, we consider the following system of DDEs with several delays:

$$\dot{x} = F(x(t), x(t - \tau_1), \dots, x(t - \tau_m), \mu), \tag{8}$$

where x is the n -dimensional vector of (physical) state variables, τ_i are the time delays ($\tau_i > 0$), μ is a k -dimensional vector belonging to the parameter space Ω , F is an n -dimensional function : $F : \Omega \times C \rightarrow \mathbb{R}^n$, with $C = C([-r, 0], \mathbb{R}^n)$, the Banach space of continuous mappings from the interval $[-r, 0]$ into \mathbb{R}^n , $r = \max_i \tau_i$. In order to integrate (8) in time, an *initial function* $\phi(\theta)$, $\theta \in [-r, 0]$ must be specified, and the solution $x(t)$ depends on the initial function ϕ , which can be made explicit by denoting the solution to (8) by $x(t, \phi)$.

The equilibrium solutions of the system of DDEs (8) are the same as those of the ODE system obtained by putting all delays τ_i equal to zero. However, the stability of equilibria of ODEs and DDEs is different. As is well known, the stability of an equilibrium x^0 of a set of ODEs $\dot{x} = f(x, \mu)$, with $x \in \mathbb{R}^n$, is determined by the eigenvalues of the Jacobian $Df = \left[\frac{\partial f_i}{\partial x_j} \Big|_{x^0, \mu^0} \right]_{ij}$, that is, by the roots of the (polynomial) characteristic equation $\det(\lambda I - Df) = 0$. For a set of DDEs (8), the *characteristic matrix* is defined as

$$\Delta(x^0, \mu^0, \lambda) = \lambda I - \sum_{i=0}^m A_i(x^0, \mu^0) e^{-\tau_i \lambda}, \quad (9)$$

where x^0 is an equilibrium of (8) for $\mu = \mu^0$, I is the $n \times n$ identity matrix, $\tau_0 = 0$ and

$$A_i = \frac{\partial F}{\partial x(t - \tau_i)} \Big|_{x^0, \mu^0}. \quad (10)$$

Note that the right hand side of (8) can thus be written as

$$F(x(t), x(t - \tau_1), \dots, x(t - \tau_m), \mu^0) = \sum_{i=0}^m A_i(x^0, \mu^0) x(t - \tau_i) + f(x(t), x(t - \tau_1), \dots, x(t - \tau_m), \mu^0) \quad (11)$$

where f only contains nonlinear terms. Again, the stability is determined by the eigenvalues λ , which are the roots of the *characteristic equation* $\det(\Delta(x^0, \mu^0, \lambda)) = 0$. This equation is much harder to solve than that for the ODE case, since it contains exponential factors in the unknown λ . The transcendental characteristic equation has infinitely many roots, as opposed to the polynomial characteristic equation for a set of ODEs that has only n roots. For τ going to zero, the real parts of all but n eigenvalues of the DDE system go to $-\infty$ (see also [3] and [1]).

For our particular system (7) the stability is determined by the roots of the following equation :

$$\det(\lambda I - A_0(x^0, \mu^0) - A_1(x^0, \mu^0) e^{-\tau \lambda}) = 0 \quad (12)$$

with

$$A_0 = \begin{bmatrix} \frac{3}{2}(1 - \phi^2) - 3R & -1 & -3\phi \\ \frac{1}{\beta^2} & \frac{1}{2\beta^2} \left(\frac{\Gamma - \Gamma}{\sqrt{\Psi}} - \frac{\Gamma_0 + k(\Psi - \Psi_s)}{\Psi} \right) & 0 \\ -2\sigma R\Phi & 0 & \sigma(1 - \Phi^2 - 2R) \end{bmatrix}, \quad (13)$$

and

$$A_1 = \begin{bmatrix} 0 & 0 & 0 \\ \frac{1}{\beta^2} \left(k \frac{\partial \Psi_s}{\partial \Phi} \right) & \frac{1}{\beta^2} \left(\frac{\Gamma_0 + k(\Psi - \Psi_s)}{2\Psi} - k \right) & 0 \\ 0 & 0 & 0 \end{bmatrix}, \quad (14)$$

The stability of (7) was analysed with the numerical methods described in [2] and [5]. These methods allow to compute those eigenvalues that are critical for the stability (i.e., the eigenvalues with largest real part) within a continuation context.

With these continuation techniques, we investigate how the stability changes as the delay is varied. Figure 2 indicates how the rightmost eigenvalues change as a function of the delay τ for the two equilibria corresponding to $\Gamma = 1.1$. For both equilibria, one eigenvalue is not affected by the delay (the horizontal lines in Fig. 2). All remaining curves represent complex pairs of eigenvalues. Both equilibria exhibit a complex pair of eigenvalues moving through the imaginary axis as τ is increased, corresponding to a Hopf bifurcation.

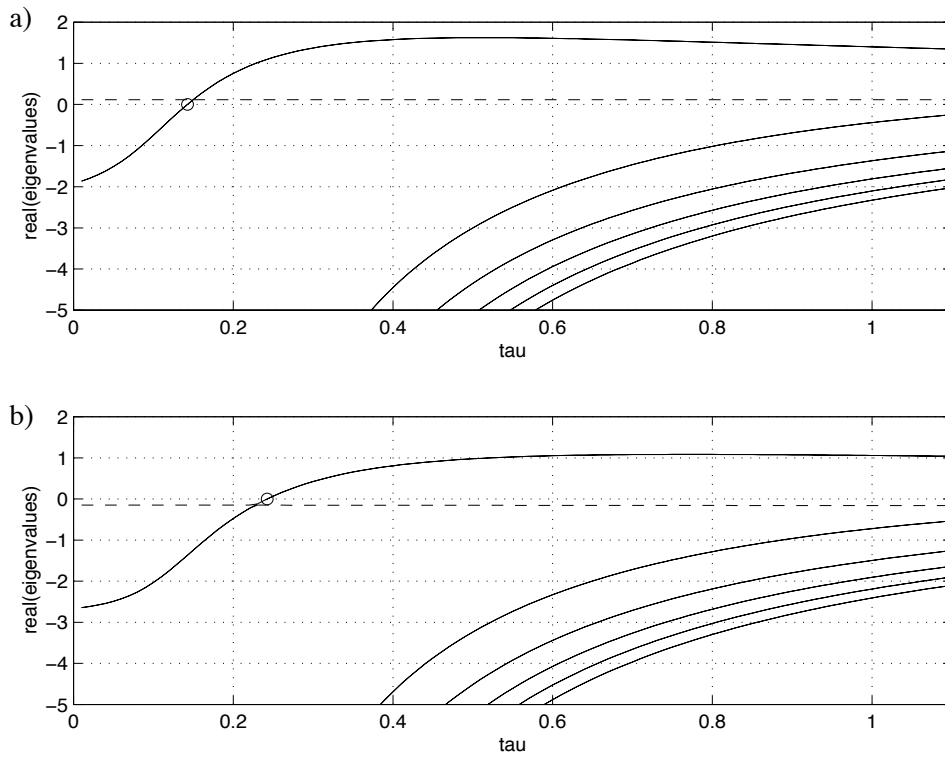


Figure 2: Evolution of the real part of the rightmost eigenvalues of the characteristic equation for respectively, a) the no-stall equilibrium, b) the stall equilibrium, corresponding to $\Gamma = 1.1$. Solid lines indicate complex pairs of roots, dashed lines indicate real roots. The Hopf bifurcations are indicated with 'o'.

3.2 Continuation of Hopf points

A Hopf bifurcation occurs at an equilibrium (x^H, μ^H) of (7) for which the characteristic equation has a single pair of purely imaginary roots $\lambda = \pm i\omega^H$. Hence the following equation has to be fulfilled :

$$\det(\pm i\omega^H I - A_0(x^0, \mu^0) - A_1(x^0, \mu^0)e^{\mp i\tau\omega^H}) = 0 \quad (15)$$

We can again use continuation techniques [2] to find branches of Hopf points in the two-parameter space (Γ, τ) . From equation (15) it is easy to see that if a Hopf bifurcation occurs for $\tau = \tau_0$, with eigenvalue $\lambda = \pm i\omega^H$, then there will be Hopf bifurcations with the same value of ω for all values τ_n satisfying

$$\tau_n = \tau_0 + \frac{2n\pi}{\omega^H}, \quad n = 1, 2, \dots$$

This phenomenon is illustrated in Fig. 3, which shows the computed branches of Hopf points starting from the Hopf bifurcations shown in Fig. 2. It seems that no other Hopf bifurcations occur for moderate values of τ . This infinitude of Hopf bifurcations is of course impossible in the (finite-dimensional) first order model, unless other bifurcations occur in between. A second difference with the first order model is the fact that there are also Hopf bifurcations to the right of Γ_{peak} . This means that if τ was taken as large as 1, as is done in [4], the equilibria to the right of Γ_{peak} would also have destabilized. Further investigation showed that these Hopf bifurcations also occur in a second order model. This result is not further investigated in the following section on periodic solutions,

because the analysis of the periodic solutions emanating from the Hopf bifurcations to the left of Γ_{peak} prevents us from taking τ larger than 0.4. In this case the equilibria to the right of Γ_{peak} are still stable.

The discontinuity of the curve at $\Gamma = \Gamma_{peak}$ is due to the fact that the term $\Psi_s(\Phi)$ in the S-control law has a discontinuous derivative at the peak (see Fig. 1).

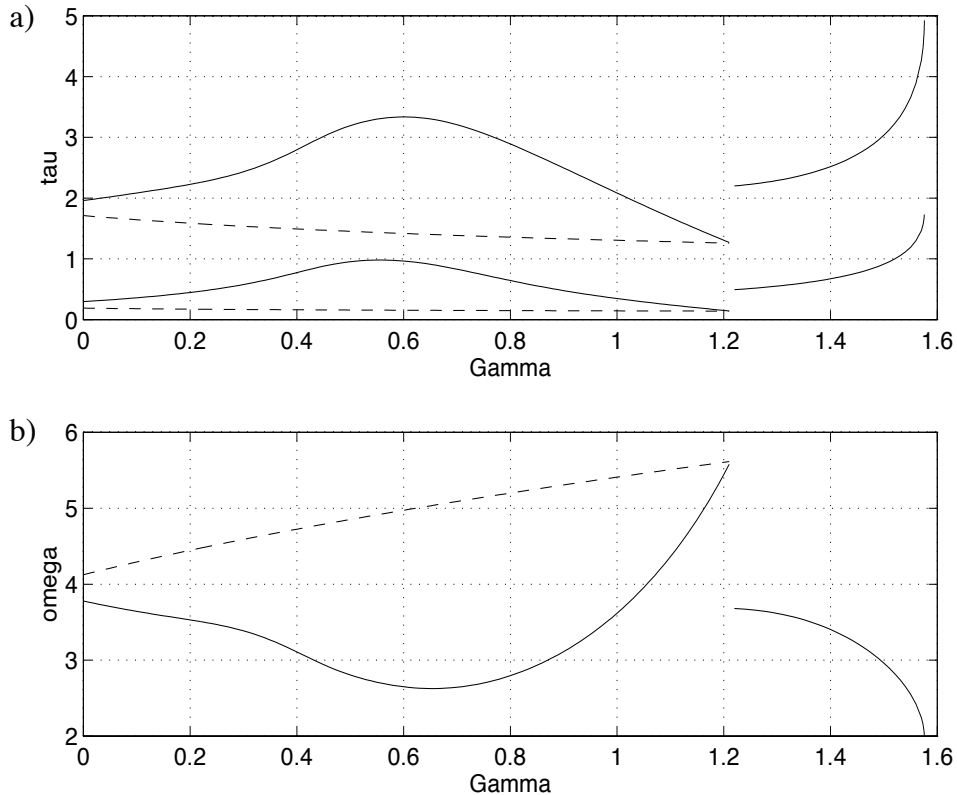


Figure 3: a) Location of Hopf bifurcations in (Γ, τ) -space. Solid lines indicate Hopf bifurcations on Ψ_s , dashed lines indicate Hopf bifurcations on Ψ_u . b) Value of ω^H for the Hopf points in a). Solid lines indicate ω^H on Ψ_s , dashed lines indicate ω^H on Ψ_u .

3.3 Analysis of periodic solutions

A periodic solution of an (autonomous) ODE is completely characterised by one initial point, say $x(0)$, on the limit cycle, satisfying the periodicity condition $x(0) = x(T)$ with T the period. Since the solution of a DDE of the form (8) depends on the initial *function* $\phi(\theta)$, $\theta \in [-r, 0]$, a periodic solution of (8) is determined by a function $x(\theta)$ such that $x(\theta) = x(T + \theta)$ for all $\theta \in [-r, 0]$ and period T . We can define the Poincaré operator P , which associates with each initial function ϕ the function $P\phi = x_T(\phi)$ where $x_T(\phi)$ is the segment of the solution $x(T + \theta, \phi)$, $-r \leq \theta \leq 0$. A periodic solution can then be characterised by an initial function ϕ^* such that $P\phi^* = \phi^*$. We refer to [5] for details on how periodic solutions of DDEs are computed numerically.

The stability of a periodic solution of a DDE is determined by the modulus of the Floquet multipliers λ_i , i.e. the eigenvalues of the *linearized* Poincaré operator S defined by

$$S\Delta\phi = y_T(\Delta\phi).$$

Here $y_T(\Delta\phi)$ is the solution on $[T - r, T]$ of the variational equation

$$\frac{dy}{dt} = \sum_{i=0}^m f_i(x^*(t, \phi), x^*(t - \tau_1, \phi), \dots, x^*(t - \tau_m, \phi))y(t - \tau_i)$$

with initial function $\Delta\phi$, where f_i denotes the derivative of the right hand side with respect to $x(t - \tau_i)$. This equation is obtained by linearizing equation (8) around the reference solution $x^*(t, \phi)$.

For a periodic solution of a DDE there is an infinite number of Floquet multipliers, but they all have finite multiplicity and zero is the only cluster point. Furthermore, there is always a (trivial) Floquet multiplier $\lambda = 1$. A periodic solution is stable if all Floquet multipliers (except the trivial one) have modulus smaller than one.

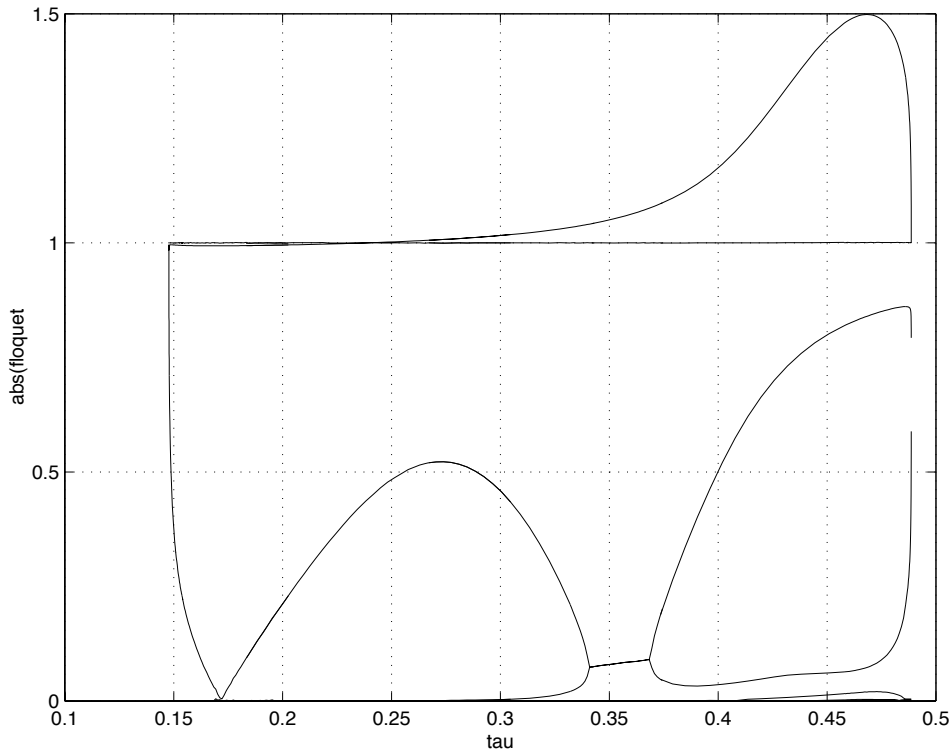


Figure 4: Evolution of the dominant Floquet multipliers of the periodic solution emanating from the stalled equilibrium corresponding to $\Gamma = 1.206$

Continuation of periodic solutions of the model (7) and analysis of their stability by computing the dominant Floquet multipliers were done with the software described in [5]. Figure 4 illustrates a typical output of the numerical software. What is plotted is the evolution of the dominant Floquet multipliers as a function of τ for the limit cycle emanating from the stalled equilibrium for $\Gamma = 1.206$, thus providing the necessary information for the stability and the bifurcation analysis. If we define $\tau_c = 0.2375$, the numerical analysis leads to the following conclusions. For $\tau < \tau_c$, the limit cycle is stable (no Floquet multipliers larger than one in modulus). At $\tau = \tau_c$, a real Floquet multiplier moves through 1, indicating that the limit cycle undergoes a transcritical bifurcation. This means that the limit cycle coalesces with another limit cycle and loses its stability to the other one. As a result, the limit cycle itself is unstable for $\tau > \tau_c$.

For the particular application that we study, not only the stability of the limit cycle is important, but also its position in state space. Since state space pictures are clearer for most readers, we will from now on display most of the results in state space. When taking into account both stability and position of the limit cycle, it seems that we have to make a distinction between the cases $\tau < 0.4$ and $\tau > 0.4$.

3.3.1 The case $\tau < 0.4$.

The results here are very similar tho those for the system with first order lag. When Γ is chosen slightly smaller than Γ_{peak} , we have two equilibria, one on the stall characteristic and one on the no-stall characteristic. Both undergo a Hopf bifurcation when τ is increased. The limit cycle that emanates from the stalled equilibrium (further called the *stall limit cycle*) is stable, the one that emanates from the no-stall equilibrium (further called the *no-stall limit cycle*) is unstable. The evolution of the stall limit cycle for increasing τ is sketched in Fig. 5. Just after the Hopf bifurcation, the stall limit cycle grows in size if τ is increased, while it retains approximately the same distance from the $R = 0$ plane. As τ is increased further, the stall limit cycle shrinks in size and moves down towards the $R = 0$ plane, while remaining stable. At $\tau = \tau_c$ (see also Fig. 4 and the explanation there), it undergoes a transcritical bifurcation and exchanges stability with the no-stall limit cycle. For larger values of τ , the stall limit cycle is located in the nonphysical region $R < 0$ and thus needs no further attention. For $\tau > \tau_c$, it is the no-stall limit cycle that is stable. This limit cycle is located in the $R = 0$ plane, and stays very small in size as τ is further increased, as can be seen from Fig. 6.

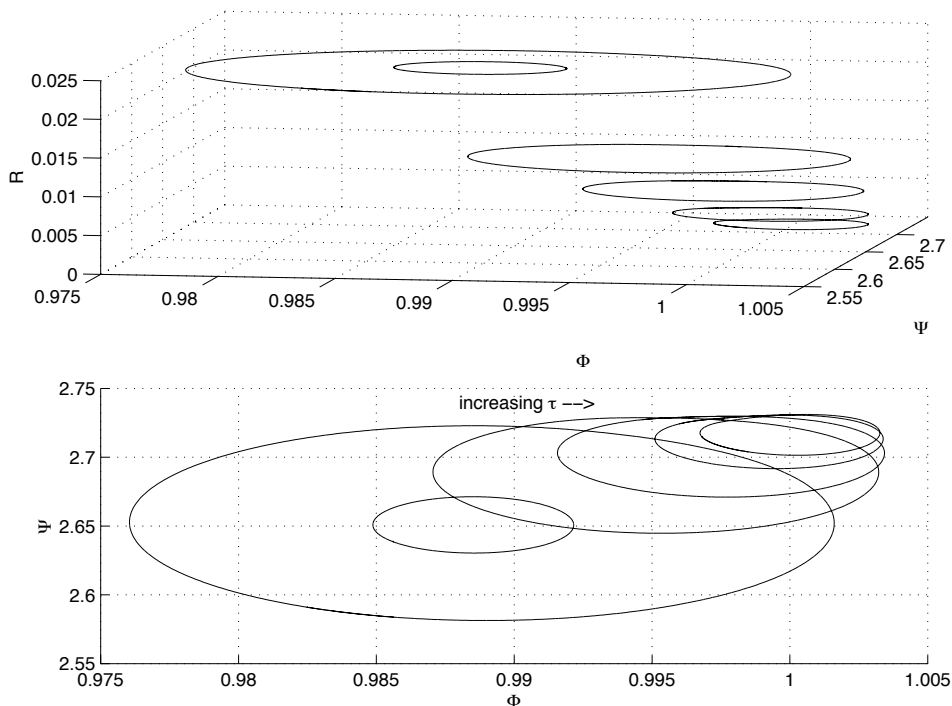


Figure 5: Evolution of the periodic solutions in state space for increasing τ , $\tau < \tau_c$.

3.3.2 The case $\tau > 0.4$.

For larger values of τ , the results start to diverge from those for the first order model. First of all, although the no-stall limit cycle retains its stability, it grows rapidly in size when τ is increased (Fig. 6) which means its physical properties are less desirable. Furthermore, the limit cycle has a turning point for $\tau \approx 0.42$, so there is no stable limit cycle left for $\tau > .42$. This is fundamentally different from the model with a first order lag, where the no-stall limit cycle persists for values of τ up to $\tau = 1$, while retaining its desirable small size.

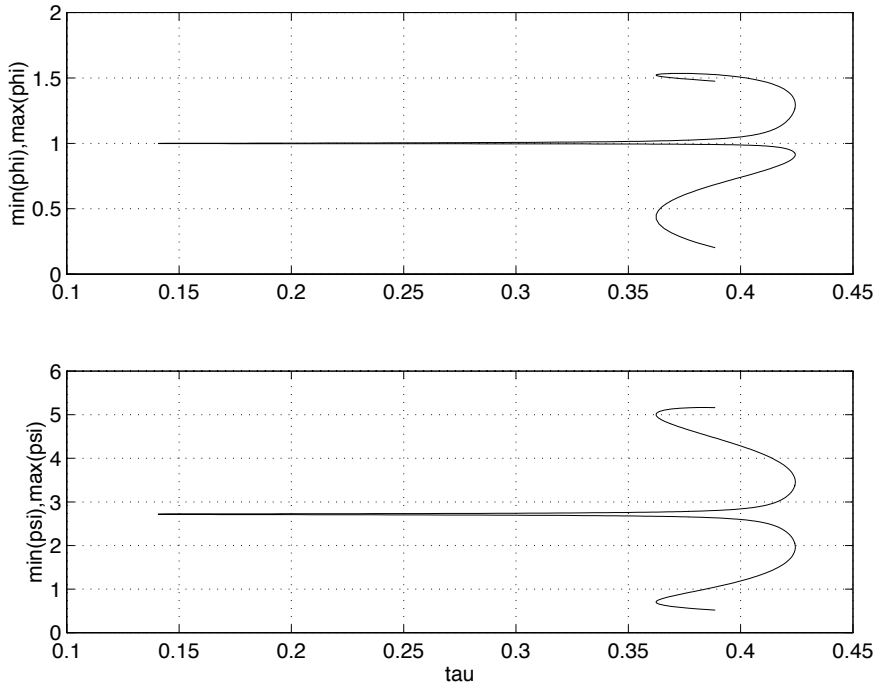


Figure 6: Minimum and maximum values attained by the periodic solution emanating from the no-stall equilibrium corresponding to $\Gamma = 1.206$, as a function of the delay τ

The analysis above assumes a 0.5% error on the optimal value for Γ , Γ_{peak} , that is, $\Gamma = 1.206$. The conclusions would be different for smaller values of Γ (corresponding to larger errors on Γ_{peak}), because the stall limit cycle then grows in size and moves away from the $R = 0$ plane as τ is increased. However, as in the first order case, numerical experience reveals that the desirable phenomena obtained for Γ close to Γ_{peak} persist over a larger range when the control action is (rather severely) saturated. A bifurcation analysis in the presence of saturation confirms this experience. In this case also other phenomena (e.g. period doublings) which are parameter-sensitive, are observed, but they are not presented in this paper.

4 Conclusion

We have studied the S-control law for the Moore-Greitzer axial compressor model, assuming that the control enters through a time-delay. The resulting system of delay differential equations is studied by means of numerical bifurcation analysis. The results can be seen as an extension of those obtained in Larsen et al. [4], where it was assumed that the control enters through a first order lag.

For small values of the delay, the delayed control is shown to stabilize a small limit cycle at a desirable location, whereas a static implementation of the controller would stabilize an equilibrium point with less desirable physical properties. These results are very similar to those presented in Larsen et al. [4] for the system with first order lag. For larger values of the delay, the results start to diverge from those for the first order model, i.e. the stable limit cycle becomes large in state space (which is undesirable) and has a turning point, so that no stable limit cycle exists for large values of the delay.

Acknowledgements

This paper presents research results of the Belgian Programme on Interuniversity Poles of Attraction, initiated by the Belgian State, Prime Minister's Office for Science, Technology and Culture (IUAP P4/02). The scientific responsibility rests with its authors.

References

- [1] O. Diekmann, S. A. van Gils, S. M. Verduyn Lunel, and H.-O. Walther. *Delay Equations, Functional-, Complex-, and Nonlinear Analysis*, volume 110 of *Applied Mathematical Sciences*. Springer-Verlag, 1995.
- [2] K. Engelborghs and D. Roose. Numerical computation of stability and detection of Hopf bifurcations of steady state solutions of delay differential equations. Report TW 274, Dept. of Computer Science, KULeuven, January 1998.
- [3] J. K. Hale and S. M. Verduyn Lunel. *Introduction to Functional Differential Equations*, volume 99 of *Applied Mathematical Sciences*. Springer-Verlag, 1993.
- [4] M. Larsen, B. Collier, R. Sepulchre, and P. V. Kokotović. Dynamic control of axial compressors. In *Proceedings of the 6th IEEE Conference on Control Applications*, pages 663–670. IEEE, 1997.
- [5] T. Luzyanina, K. Engelborghs, K. Lust, and D. Roose. Computation, continuation and bifurcation analysis of periodic solutions of delay differential equations. *International Journal of Bifurcation and Chaos*, 7(11):2547–2560, november 1997.
- [6] F. K. Moore and E. M. Greitzer. A theory of post-stall transients in axial compressors: Part I - development of the equations. *AMSE Journal of Engineering for Gas Turbines and Power*, 108:68–76, 1986.
- [7] R. Sepulchre and P. V. Kokotović. Asymptotic methods for nonlinear control: a jet engine case study. UCSB Technical Report CCEC-960220, University of California at Santa Barbara, 1996.